Medicinal Chemistry & Drug Discovery

Role of Anomalous Water Constraints in the Efficacy of Pharmaceuticals Probed by 1H Solid-State NMR

Joshua T. Damron+,[a] Kortney M. Kersten+,[a] Manoj Kumar Pandey,[b] Yusuke Nishiyama,[b, c] Adam Matzger,*[a, d] and Ayyalusamy Ramamoorthy*[a, e]

Water plays a complex and central role in determining the structural and reactive properties in numerous chemical systems. In crystalline materials with structural water, the primary focus is often to relate hydrogen bonding motifs to functional properties such as solubility, which is highly relevant in pharmaceutical applications. Nevertheless, understanding the full electrostatic landscape is necessary for a complete structure-function picture. Herein, a combination of tools including 1H magic angle spinning NMR and X-ray crystallography are employed to evaluate the local landscape of water in crystalline hydrates. Two hydrates of an anti-leukemia drug mercaptopurine, which exhibit dramatically different dehydration temperatures (by 90 °C) and a three-fold difference in the in vivo bioavailability, are compared. The results identify an electrosteric caging mechanism for a kinetically trapped water in the hemihydrate form, which is responsible for the dramatic differences in properties.

Hydrates are crystalline materials where water molecules occupy a regular space within the crystal structure, whether at an isolated site or within a defined channel.[1] For cases where the crystal structure is lost during application, such as with the dissolution of pharmaceutical hydrates, it might be expected that the presence of water in the solid would have little influence on properties. To the contrary, approximately 20 % of the 100 top selling drugs are hydrated forms (See Tables S1 and S2 in the supporting information) and their physicochemical properties often differ dramatically from their anhydrous counterparts.[1,2] Inclusion of water into the crystalline lattice typically decreases the water solubility of that form due to the partial solvation of molecules in the solid state.[1] Reduced solubility of hydrate forms is also regularly accompanied by increased resistance to solid form changes occurring during production and storage.[1] Consequently, the choice of a hydrate form for development often involves a tradeoff between solubility and stability[3] which can reduce the efficacy of BCS class II and IV drugs where bioavailability can be solubility limited.[4] The increased stability seen in these hydrate forms largely arises from hydrogen bonding throughout the crystal structure between the pharmaceutical and water molecules.[5] Determining the propensity for hydrate formation based on the available number of hydrogen bond donors and acceptors in a molecule,[6,7] as well as predicting the stability of a structure based on the hydrogen bonding motif surrounding the water molecules[5,8] have been pursued in the literature. Nevertheless, hydrogen bonding is only one of the aspects related to hydrate stability; the participation of other electrostatic interactions and assembly modes merit consideration.

The most commonly used technique to examine hydrogen bonds in the solid-state is X-ray crystallography,[7] despite the challenge of low electronic density around the 1H nucleus. In solution, 1H NMR spectroscopy is employed to elucidate the strength of hydrogen bonding interactions and is often used to determine secondary structure in biological macromolecules. 1H solid state (SS) NMR spectroscopy is ideally suited for providing chemical information to supplement the structural picture arising from crystallography,[9] although historically the technique has been severely limited due to issues caused by very large homogenous 1H/1H dipolar couplings facilitating spin diffusion and severe spectral broadening. In recent years, advances in magic angle spinning (MAS) NMR technology, which is now capable of 120+ kHz sample spinning frequencies, have made 1H SS NMR in rigid proton systems far more informative through the significant suppression of these dipolar couplings.[10] They have also enabled a burst of methodological development, including recently proposed pulse sequences to measure 2D 1H/1H anisotropic/isotropic chemical shift (from here on referred to as CSA/CS) correlations.[11–14] A recent application of such a sequence was successfully used to refine hydrogen bond positions in L-ascorbic acid.[15] The achieved

[a] J. T. Damron,+ K. M. Kersten,+ Dr. A. Matzger, Dr. A. Ramamoorthy
Department of Chemistry
University of Michigan
930 N. University Ave., Ann Arbor, MI 48109-1055, USA
E-mail: ramamoor@umich.edu
matzger@umich.edu

[b] M. K. Pandey, Dr. Y. Nishiyama
RIKEN CLST-JEOL
Collaboration Center RIKEN Yokohama,
Kanagawa 230-0045, Japan

[c] Dr. Y. Nishiyama
JEOL RESONANCE Inc Musashino,
Akishima, Tokyo 186-8558, Japan

[d] Dr. A. Matzger
Macromolecular Science and Engineering
University of Michigan
2300 Hayward Avenue, Ann Arbor, MI 48109-1055, USA

[e] Dr. A. Ramamoorthy
Biophysics Program
University of Michigan
930 N. University Ave., Ann Arbor, MI 48109-1055, USA

[+] These authors contributed equally.

Supporting information for this article is available on the WWW under https://doi.org/10.1002/slct.201701547

atomic resolution by fast MAS makes the ^{1}H chemical shift anisotropy tensor highly diagnostic of the electronic environment of the nucleus. This approach should serve as a direct measure of water binding interactions in hydrate structures to augment the X-ray data. This potentiality is realized here in the context of pharmaceutical hydrates.

One dramatic example of the role of water in pharmaceuticals is the recently discovered hemihydrate form of the anti-leukemia drug, mercaptopurine.[16] This form shows a ~3 fold increase in the bioavailability of the drug over the currently prescribed monohydrate form, a feature that results from a combination of several physical properties. Of the three forms of mercaptopurine, the anhydrate form is the most soluble, as is common with hydrated materials. However, the anhydrate form suffers from conversion to the least soluble (monohydrate) form in aqueous solution within hours, whereas the hemihydrate form is more stable and does not completely convert for several days.[16] The monohydrate has a dehydration temperature of 150 °C, whereas the hemihydrate form shows an exceptionally high dehydration temperature of 240 °C. This value is the highest observed for any non-salt hydrate in the literature,[17–21] and a staggering 90 °C higher than the monohydrate form. Consequentially, an ideal balance of stability and solubility is found in the hemihydrate form that is responsible for its increased efficacy. Given the extreme thermal stability, which is generally indicative of high thermodynamic stability, the favorable dissolution and increased bioavailability of the hemihydrate is an exception to typical hydrate behavior. The structural basis for this kinetic behavior is elucidated here and aspects of the thermodynamics leading to the observed physical properties of each form are computed. To probe the factors that contribute to the structural variation of water and its environment, we chose to investigate the local environment of water in the two hydrates of mercaptopurine due to the significant differences in stability and efficacy known for the mono and hemihydrate forms. The combined use of the ^{1}H CSA measured from MAS experiments, IR experiments, and quantum calculations as presented below enabled us to develop a mechanism for the dehydration behavior and functional difference between these two forms of mercaptopurine hydrates.

Structural depictions based on the reported crystal structures[16] emphasizing the incorporation of water in the two hydrate forms of mercaptopurine are shown in Figure 1b. In the monohydrate, water molecules participate in an extended hydrogen bond network with each water bridging three mercaptopurine molecules. The hydrogen bond distances, based on crystal structures with protons normalized to average neutron scattering positions, for O—H···N, O—H···S and N—H···O are 1.82 Å, 2.40 Å, and 1.75 Å, respectively. In the hemihydrate structure, six mercaptopurine molecules are hydrogen bound through N—H···N bonds between the imidazole and pyrimidine moieties forming ring-like structures. The water molecules sit inside the ring with its oxygen weakly interacting with the aromatic ring via C—H···O interactions (at H···O distances of 2.28 Å and 2.42 Å), while the hydrogens participate in O—H···S hydrogen bonds with sulfur atoms in adjacent rings above and below at distances of 2.37 and 2.45 Å (Figure 1b). The
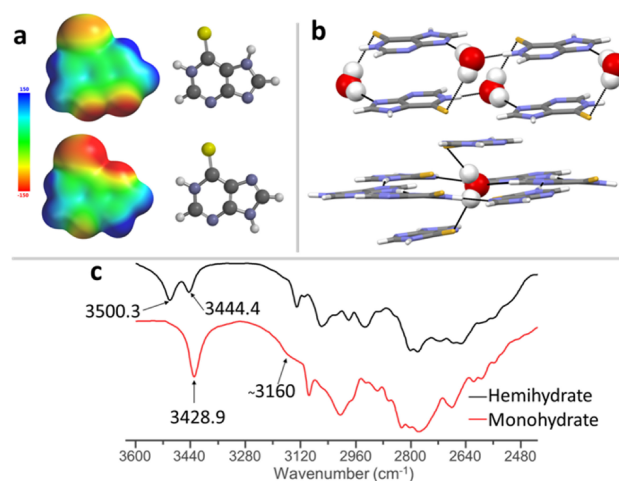

Figure 1. Effect of tautomerization and hydration on mercaptopurine structure. (**a**) Electrostatic potential maps of the mercaptopurine tautomers seen in the monohydrate (top) and hemihydrate (bottom) forms. (**b**) Depictions of the hydrogen bonding motifs within the monohydrate (top) and hemihydrate (bottom) structures. (**c**) IR spectrum showing the OH stretching frequencies of the two forms of mercaptopurine.

preference for hydrogen bonding positions are reflected by the electrostatic potential map of mercaptopurine show in Figure 1a, where the tautomerization redistributes the charge density across the molecule. X-ray analysis allows one to infer chemical information such as hydrogen bonding based on atomic positions, however, it does not always reflect the exact type or magnitude of the interactions occurring. On the other hand, ^{1}H SS NMR is sensitive to the electrostatic environment of each atom and can provide additional information regarding the type and magnitude of the interactions involved.

The 2D CS/CSA 1H MAS spectra of both mercaptopurine hydrates, obtained using the pulse sequence given in Figure S1 of the supporting information, are shown in Figure 2 and the corresponding NMR parameters are summarized in Table 1. For

Table 1. Isotropic and anisotropic chemical shift parameters for protons in hemihydrate and monohydrate forms of mercaptopurine measured from fast magic angle spinning solid-state NMR experiments.

Hemihydrate	NH	NH	Ar	H2O
δ_{iso} (ppm)	15.17	13.23	8.34	2.75
ζ (ppm)	10.2	11.6	5.2	9.6
η	0.75	0.8	0.85	0.6
Monohydrate	NH	Ar	H2O	
δ_{iso} (ppm)	14.4	8.45	5.9	
ζ (ppm)	11.3	5.5	10.2	
η	0.7	0.85	0.75	

the hemihydrate, the NH proton signals are resolved at 13 and 15 ppm, the unresolved aromatic resonances appear at 8.34 ppm, and the water signal is at 2.75 ppm. Discussion of the NMR assignments is given in the supporting information
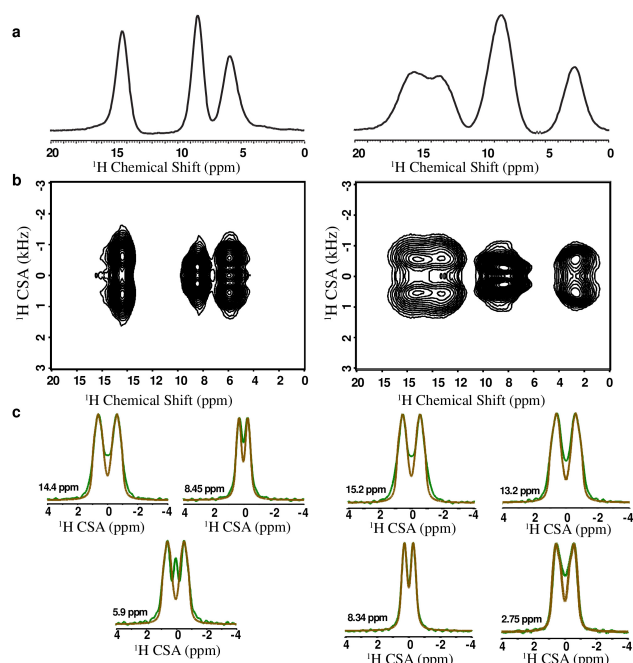
Figure 2. [1]H chemical shift anisotropy spectra of monohydrate (left) and hemihydrate (right) of mercaptopurine. (**a**) 1D isotropic ^{1}H spectra collected under 90 kHz MAS. (**b**) 2D ^{1}H CS/CSA correlation spectra obtained using the RF pulse sequence given in ESI Figure S1. (**c**) ^{1}H CSA lineshapes, extracted from 2D ^{1}H CS/CSA spectra (green), associated with the indicated isotropic chemical shift values, and their simulated best fits obtained using SIMPSON (brown). All other experimental details are given in the Supporting Information.

with Figures S2 and S3 and Table S3. For the monohydrate, the water peak appears at 5.9 ppm, the overlapping NH peaks appear at 14.4 ppm, and the aromatic protons at 8.45 ppm. It is typical in a hydrogen bond for the nucleus to be pulled from the center of mass of the electrons of the atom,[22] which results in a deshielded nucleus, larger isotropic CS values and an increase in the CSA.[23–26] Proximate electron rich groups can also cause dramatic CS changes, depending on the atomic species, orientation, etc.[27] Consistent with the X-ray data, stronger hydrogen bonding for the monohydrate water is evidenced by the 0.6 ppm larger CSA and 3 ppm further downfield isotropic CS. The 3 ppm difference in the isotropic CS of the water resonance between the two forms indicates dramatically different local environments for the water. For reference, the CS of pure water at ambient conditions is 4.72 ppm, which is downfield shifted due to transient hydrogen bonding from dilute or "monomeric" values typically around 1 ppm.[28–30] The rigid hydrogen bonding in the monohydrate results in more deshielding by slightly more than 1 ppm. On the other hand, a large up-field shift is observed for the hemihydrate, supportive of weaker hydrogen bonding, and/or a combination of intermolecular electronic shielding from the immediate solid environment. The hemihydrate water is surrounded by a dense electronic environment of 4 sulfur atoms and neighboring aromatic rings. These sulfur atoms and

the neighboring aromatic moieties form a tight "cage" around the water molecules, providing the electronic shielding.

The differing water environments between the two forms are also implicated by IR spectroscopy. Two OH stretches are observed for the hemihydrate (3500.3 and 3444.4 cm^{-1}) while only one OH stretch for the monohydrate (3428.9 cm^{-1}) is observed in the 3300–3600 cm^{-1} region (Figure 2c). The monohydrate stretch appears at a lower energy which is consistent with the structure having stronger hydrogen bonding.[5,31] Computational predictions (Figure S4-S8 in the supporting information) of the stretching frequencies are in accord with these experimental observations but also detect an additional OH stretch at an even lower energy of ~3160 cm^{-1} belonging to the hydrogen bound with the nitrogen. No corresponding stretches are seen in the hemihydrate form. The IR data supports the assertion that the two forms display distinctive hydrogen bonding that is stronger in the monohydrate form.

No clear explanation for the difference in dehydration temperatures, which is much higher for the hemihydrate, can be identified from the data above. Consequently, we performed molecular mechanics and DFT calculations taking each of the structures with and without the water molecules present to compute the theoretical desolvation energy for each hydrate form (Figure S9 in the supporting information). Consistent with the experimental data, the energy of removal per water molecule is higher for the monohydrate (on the order of 10 kcal/mol/water molecule), suggesting that the hydrogen bonding in the monohydrate is the dominant enthalpic factor between the two (See Tables S4 and S5 in the supporting information). Again, neither experimental nor computational data evidence any specific binding interaction accounting for the dramatic stability of the hemihydrate over the monohydrate form. The implication is that the high thermal stability in the hemihydrate water is due to the constrained environment imposed by the electronically dense neighbors mimicking a cage and entrapping the water. Such a cage could explain the up field 2.75 ppm isotropic chemical shift value. This large upfield shift strongly corroborates a tight electrosteric environment due to magnetic shielding of the cage, despite the presence of hydrogen bonding between the water and the hemihydrate structure.

The above information suggests the following hypothesis for the dehydration mechanism in each form. Upon heating and water loss, the monohydrate becomes amorphous due to the collapse of the extensive network around the water molecules in the structure.[16] The molecules then undergo tautomerization followed by recrystallization into the anhydrate form. The hemihydrate however, converts immediately to the structurally similar anhydrate upon water loss shortly before decomposition, with no intermediate amorphous phase.[16] This occurs through a thermal loosening of the "cage", which is dependent on the hydrogen bonding between the mercaptopurine molecules themselves and not from a specific interaction of the water molecules within the crystal. Functionally, the electro-steric cage containing weakly interacting water provides only a minor decrease to the solubility of the form

compared to the anhydrate, but has a great impact on the stability of the form overall, leading to the hemihydrate being the most efficacious solid form of mercaptopurine.

In conclusion, ^{1}H SS NMR effectively characterizes the environment of water molecules in the solid state to provide unique information about the role of intermolecular interactions on pharmaceutical hydrate properties; as demonstrated in this study, combined with crystal structures and theoretical computation, the ^{1}H MAS SS NMR experiments can probe electrostatic interactions around H atoms. Though typically the role of hydrogen bonding is considered dominant, using fast ^{1}H MAS SS NMR methodology and computation, we propose a mechanism for the outstanding stability of the hemihydrate form of mercaptopurine being due to a structural cage imposed on the contained water molecules. This provides a molecular rationale for the favorable balance of stability and solubility of the hemihydrate form of mercaptopurine. In addition, it indicates a potential design route wherein creating similar caged or kinetically trapped waters could supply an avenue to more efficacious drugs.

Supporting Information Summary

Detailed descriptions of the experimental procedures for the sample preparation, NMR and IR can be found in the supporting information. The setup of the model for the DFT calculations is also described. In addition, any supporting data regarding NMR assignments, energy values or IR assignments is provided.

Conflict of Interest

The authors declare no conflict of interest.

[1] R. K. Khankari, D. J. W. Grant, *Thermochim. Acta* **1995**, *248*, 61–79.
[2] F. Tian, H. Qu, A. Zimmermann, T. Munk, A. C. Jørgensen, J. Rantanen, *J. Pharm. Pharmacol.* **2010**, *62*, 1534–1546.
[3] D. Giron, C. Goldbronn, M. Mutz, S. Pfeffer, P. Piechon, P. Schwab, *J. Therm. Anal. Calorim.* **2002**, *68*, 453–465.
[4] G. L. Amidon, H. Lennernäs, V. P. Shah, J. R. Crison, *Pharm. Res.* **1995**, *12*, 413–420.
[5] K. R. Morris, N. Rodriguez-Hornedo, in *Encyclopedia of Pharmaceutical Technology* (Eds.: J. Swarbrick, J. C. Boylan), Marcel Dekker Inc., New York, **1993**, pp. 393–440.
[6] L. Infantes, L. Fábián, W. D. S. Motherwell, *CrystEngComm* **2007**, *9*, 65–71.
[7] K. Fucke, J. W. Steed, *Water* **2010**, *2*, 333–350.
[8] A. L. Gillon, N. Feeder, R. J. Davey, R. Storey, *Cryst. Growth Des.* **2003**, *3*, 663–673.
[9] C. Martineau, *Solid State Nucl. Magn. Reson.* **2014**, *63*, 1–12.
[10] Y. Nishiyama, *Solid State Nucl. Magn. Reson.* **2016**, *78*, 24–36.
[11] M. K. Pandey, M. Malon, A. Ramamoorthy, Y. Nishiyama, *J. Magn. Reson.* **2015**, *250*, 45–54.
[12] H. K. Miah, D. A. Bennett, D. Iuga, J. J. Titman, *J. Magn. Reson.* **2013**, *235*, 1–5.
[13] G. Hou, R. Gupta, T. Polenova, A. J. Vega, *Isr. J. Chem.* **2014**, *54*, 171–183.
[14] R. Zhang, K. H. Mroue, A. Ramamoorthy, *J. Chem. Phys.* **2015**, *143*, 144201.
[15] H. K. Miah, R. Cresswell, D. Iuga, J. J. Titman, *Solid State Nucl. Magn. Reson.* **2017**, DOI 10.1016/j.ssnmr.2017.02.002.
[16] K. M. Kersten, A. J. Matzger, *Chem. Commun.* **2016**, *52*, 5281–5284.
[17] H. D. Clarke, K. K. Arora, H. Bass, P. Kavuru, T. T. Ong, T. Pujari, L. Wojtas, M. J. Zaworotko, *Cryst. Growth Des.* **2010**, *10*, 2152–2167.
[18] N. Variankaval, C. Lee, J. Xu, R. Calabria, N. Tsou, R. Ball, *Org. Process Res. Dev.* **2007**, *11*, 229–236.
[19] M. Karanam, A. R. Choudhury, *Cryst. Growth Des.* **2013**, *13*, 1626–1637.
[20] T. N. P. Nguyen, K. J. Kim, *Ind. Eng. Chem. Res.* **2010**, *49*, 4842–4849.
[21] N. Mahé, B. Nicolaï, M. Barrio, M. A. Perrin, B. Do, J. L. Tamarit, R. Céolin, I. B. Rietveld, *Cryst. Growth Des.* **2013**, *13*, 3028–3035.
[22] T. Steiner, *Angew. Chem. Int. Ed.* **2002**, *41*, 48–76; *Angew. Chemie* **2002**, *114*, 50–80.
[23] C. M. Rohlfing, L. C. Allen, R. Ditchfield, *J. Chem. Phys.* **1983**, *79*, 4958–4966.
[24] Y. Suzuki, R. Takahashi, T. Shimizu, M. Tansho, K. Yamauchi, M. P. Williamson, T. Asakura, *J. Phys. Chem. B* **2009**, *113*, 9756–9761.
[25] Y. Sharma, O. Y. Kwon, B. Brooks, N. Tjandra, *J. Am. Chem. Soc.* **2002**, *124*, 327–335.
[26] L. L. Parker, A. R. Houk, J. H. Jensen, *J. Am. Chem. Soc.* **2006**, *128*, 9863–9872.
[27] J. Schmidt, A. Hoffmann, H. W. Spiess, D. Sebastiani, *J. Phys. Chem. B* **2006**, *110*, 23204–23210.
[28] B. G. Pfrommer, F. Mauri, S. G. Louie, *J. Am. Chem. Soc.* **2000**, *122*, 123–129.
[29] V. Balevicius, K. Aidas, *Appl. Magn. Reson.* **2007**, *32*, 363–376.
[30] V. G. Malkin, O. L. Malkina, G. Steinebrunner, H. Huber, *Chem.– Eur. J.* **1996**, *2*, 452–457.
[31] H. D. Lutz, in *Solid Materials*, Springer, Berlin, Heidelberg, **1988**, pp. 97–125.